

waveguide formation.⁶ The FWHM phase matching bandwidth for QPM-SHG in a LiNbO₃ waveguide is 0.5 Å cm at 788 nm, providing tunable radiation over about 50 GHz in the UV with a 3-dB variation in output power for a 1-cm device. The QPM-SHG waveguide employed for aluminum spectroscopy had a 2.3 μm domain grating period, a 4.0-mm wide, 1-cm long waveguide, and generated radiation at 394 nm with an efficiency of about 70%/W. The output power from the waveguide was about 3 mW with 2.1 mW of fundamental radiation exiting the waveguide. The near-infrared output from the ECDL was passed through a 30-dB optical isolator and coupled into the QPM-SHG waveguide using the conventional endfiring technique. The waveguide was mounted inside a compact, temperature controlled housing complete with lenses for coupling the light into and out of the waveguide. Stable coupling efficiencies about 30% were obtained.

The HCL was used as a reference to test and characterize the monitor. The UV radiation passed through the 100% amplitude modulated lamp, and was detected using a photodetector with a transimpedance amplifier in a phase-sensitive detection scheme. By sweeping the laser frequency, the line shape of the absorption was obtained. Aluminum exhibits strong absorption in the $3P_{1/2}-4S_{1/2}$ transition at 394.4 nm. There exists a hyperfine splitting of 1.5 GHz in the ground state ($3P_{1/2}$).⁷ The hyperfine splitting was not resolved in the HCL because the Doppler broadened width of each of the overlapping sublevels was wider than the splitting. The measured width of the overlapped line shape in the HCL was 6.5 GHz. Aluminum also has another transition $3P_{3/2}-4S_{1/2}$ (396 nm). Calculations of the Boltzmann distribution governed population variations of the two manifolds show that for the vast majority of deposition conditions monitoring one of these transitions is sufficient.

To apply the present system to the evaporation process, the UV radiation was delivered directly into the vacuum deposition chamber as shown in Fig. 1. Derivative spectroscopy was employed, in which the frequency of the fundamental laser was dithered at $f = 170$ Hz with an amplitude of 0.6 GHz, and the $2f$ -output from a lock-in amplifier was used for obtaining the absorption signal. The detected signal on line center is proportional to the atomic density. The correlation between the AA signal and the deposition rate was measured by a quartz crystal monitor placed directly above the frequency-doubled laser beam path. The absorption at a deposition rate of 2 Å/s was measured to be 3% for an absorption path length of 10 cm.

Closed loop operation was demonstrated in the electron-beam evaporation chamber at a rate of 2.5 Å/s. The AA signal was used in conjunction with a simple variable-set-point comparator and proportional control for feedback. The deposition rate was also compared with a chopped ion-gauge (CIG) monitor placed above the beam path. The time constant of the lock-in amplifier was 100 ms. Outputs from the AA signal and the CIG are shown in Fig. 2, showing control of the deposition rate using the AA monitor. The signal-to-noise ratio obtained in the experiments indicates that a deposition rate control accuracy of 1% at such a low rate is possible if a reference detector placed before the vacuum chamber is used to normalize the amplitude variations due to

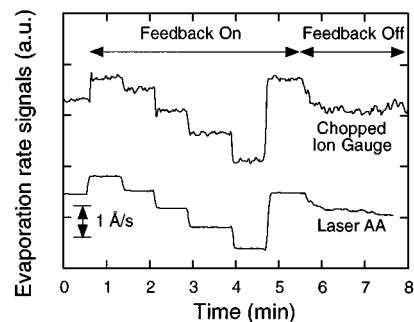


FIG. 2. Evaporation signals from the laser system under open and closed loop control along with the independent signal from the chopped ion gauge.

frequency dither and etalon effects arising from the waveguide endfaces. The increased noise on the CIG, which is presumably the actual evaporation rate, was observed during open and closed loop operation and was probably due to time-dependent variations in the evaporation plume at the location of the CIG.

The application to sputtering processes and the present system reproducibility of the UV-laser-based monitor were investigated by monitoring the deposition of aluminum in a 2 in. diam dc magnetron sputtering system. The AA monitor configuration was similar to that used in the evaporation chamber. The UV radiation passed between a 2 in. diam aluminum target and a substrate which were separated by 2 in. The absorption path length was about 5 cm. The sputtering condition included a power of 160 W, an argon pressure of 2.2 mTorr, and a background pressure of 4×10^{-6} Torr, resulting in a deposition rate of about 900 Å/min and an absorption of 20%.

Two different sets of experiments were performed to ascertain the utility of the optical probe to monitor and control of the sputtering process. First, we compared the film thickness with the overall, line-integrated AA signal; second, we compared the film thickness with the local AA signal using an aperture with a diameter of 1 cm placed between the target and the substrate and above the laser beam. Presputtering was always performed to remove the possible oxidation layer on the aluminum target. Prior to each deposition, the optical monitor was configured to yield the same signal amplitude as observed from the reference HCL. Film thicknesses were measured by masking a portion of the substrate and performing postdeposition profilometry. In each set of experiments the only independent variable was deposition time. Figure 3 shows the relationship between the time-integrated $2f$ AA signal and the thicknesses of the film with and without the aperture. The expected linear behavior for both data sets indicates that the local density of atoms in a sputtering system is correlated with the absorption, and the line integrated absorption can be used as a control variable for thickness. The relative standard deviation of the measured thicknesses was about 6% for both sets of data.

One source of the variation in the data arises due to long term drift in the AA monitor; another source are the difficulties encountered in depositing reproducible metallized aluminum films in the available sputtering system. The long term drift in the current AA monitor stems from frequency excursions in the ECDL and the etalon effects in the QPM-SHG

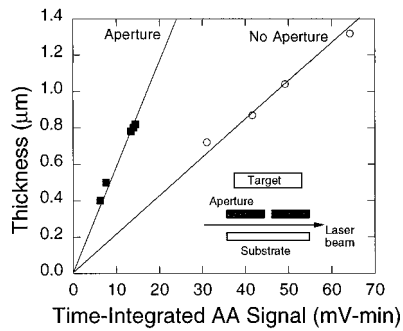


FIG. 3. Measured relation between time-integrated AA signal and thickness of the sputter coated films. The inset shows the geometry in sputtering chamber.

waveguide. The former can be corrected by locking the laser frequency to the absorption peak or by sweeping the laser frequency over the entire line shape, and the latter can be eliminated by wedging the waveguide endface. Because no attempt was made in this work to control the reproducibility of the deposition growth morphology, the nonuniformity of the sputtered film hindered reproducible film thickness measurements, although we attempted to configure the target-aperture-substrate-film thickness measurement location identically for each deposition. By improving both the stability of the monitor and the quality of the sputter coating, thickness control with a relative accuracy better than 1% can be expected, suitable for controlling metal deposition, and also for measuring the spatial distribution of the sputtered atoms.

Coherent radiation with different wavelength in the blue-UV region, suitable for AA spectroscopy of many other elements such as tungsten (385 nm), titanium (391 nm), aluminum (394 nm), gallium (403 nm), yttrium (408 nm), etc., is also available by using the present techniques. Figure 4(a) shows phasematching wavelength (λ_p) versus domain-grating period measured with a widely tunable Ti-sapphire laser. The domain-grating period, controlled by the lithographically delineated Ti film, allows SHG throughout the blue-UV region. Different widths or APE fabrication parameters for waveguides with a given domain-grating period have λ_p differing by 1–2 nm, and the temperature tuning rate of the waveguide was measured to be $0.32 \text{ \AA}/^\circ\text{C}$ as shown in Fig. 4(b), indicating that an acceptable operating temperature variation of $\pm 20^\circ\text{C}$ allows tuning to any desired atomic transition in the 380–430 nm range. The conversion efficiency of these devices ranged from 25 to 150%/W due to variations in the waveguide lithography and domain inversion grating, high enough for diode-laser-based AA spectroscopy applications.

It should be pointed out that because of the strong absorption for elements like aluminum, measurement accuracy is often limited by scale factor effects such as stray etalons, residual power, and frequency variations of the laser rather

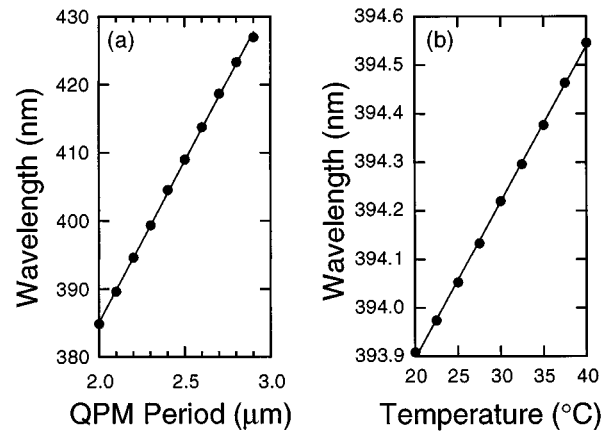


FIG. 4. (a) Measured phase matching wavelength vs QPM grating periodicity in different waveguides. (b) Measured phase matching wavelength vs temperature in a single waveguide.

than the absorption resolution of the system. When the deposition rate is high enough ($\sim 1 \mu\text{m}/\text{min}$) to produce an opaque vapor, simply detuning the laser frequency from the line center may not provide sufficient sensitivity; suitable schemes for operating in this regime are current research topics.

In summary, we have developed a frequency-doubled-diode-laser-based AA spectroscopy system for monitoring and controlling for thin-film deposition. System demonstrations were carried out for aluminum at 394 nm in both electron-beam evaporation and sputtering processes. Closed loop operation was achieved in an evaporation chamber. We have also demonstrated the possibilities of employing the laser-based system for controlling the thickness of the sputter coated films. Measuring the spatial distribution of sputtered atoms should also be possible. By using quasi-phase-matched lithium niobate waveguides, blue-UV coherent light at 380–430 nm becomes available, and useful for many technologically important elements in physical vapor deposition processes.

This work was funded by ARPA through New Focus, Inc.

- ¹S. J. Benerofe, C. H. Ahn, M. M. Wang, K. E. Kihlstrom, K. B. Do, S. B. Arnason, M. M. Fejer, T. H. Geballe, M. R. Beasley, and R. H. Hammond, *J. Vac. Sci. Technol. B* **12**, 1217 (1994).
- ²C. Lu and Y. Guan, *J. Vac. Sci. Technol. A* **13**, 1797 (1995); also preprint of presentation at the 187th Meeting of the Electrochemical Society.
- ³W. Wang, R. H. Hammond, M. M. Fejer, C. H. Ahn, M. R. Beasley, M. D. Levenson, and M. L. Bortz, *Appl. Phys. Lett.* **67**, 1375 (1995).
- ⁴M. L. Bortz, S. J. Field, M. M. Fejer, D. W. Nam, R. G. Waarts, and D. F. Welch, *IEEE J. Quantum Electron.* **30**, 2953 (1994).
- ⁵M. M. Fejer, G. A. Magel, D. H. Jundt, and R. L. Byer, *IEEE J. Quantum Electron.* **28**, 2631 (1992).
- ⁶E. J. Lim, M. M. Fejer, R. L. Byer, and W. J. Kozlovsky, *Electron. Lett.* **25**, 731 (1989).
- ⁷A. A. Radzig and B. M. Smirnov, *Springer Series in Chemical Physics* (Springer-Verlag, Berlin, 1980), Vol. 31, p. 102.